Microchimica Acta (2019) 186: 631
https://doi.org/10.1007/s00604-019-3728-7

ORIGINAL PAPER

Nanoporous platinum-copper flowers for non-enzymatic sensitive detection of hydrogen peroxide and glucose at near-neutral pH values

Hongxiao Yang[1] · Zhaohui Wang[1] · Qiuxia Zhou[1] · Caixia Xu[1] · Jiagang Hou[2]

Received: 23 March 2019 / Accepted: 1 August 2019 / Published online: 17 August 2019

Abstract

Multimodal nanoporous PtCu flowers (np-PtCu) were prepared via a two-step dealloying strategy under mild conditions. The np-PtCu alloy possesses an interconnected flower-like network skeleton with multiscale pore distribution. This material was placed on a glassy carbon electrode where it shows outstanding detection performance towards hydrogen peroxide and glucose in near-neutral pH solutions. It can be attributed to the specific structure in terms of interconnected nanoscaled ligaments, rich pore openings and a synergistic alloying effect. Figures of merit for detection H_2O_2 assay include (a) a working voltage of 0.7 V (vs. the reversible hydrogen electrode); (b) a wide linear response range (from 0.01 to 1.7 mM), and (c) a low detection limit (0.1 μM). The respective data for the glucose assay are (a) 0.4 V, (b) 0.01–2.0 mM, and (c) 0.1 μM. The method is not interfered in the presence of common concentrations of dopamine, acetaminophen and ascorbic acid.

Keywords Nanocomposite · Electrocatalyst · Electrochemical detection · Alloy · Detection performance

Introduction

Hydrogen peroxide (H_2O_2) is involved in many fields, for instance, chemical, pharmaceutical, biological, food, and environmental processes etc. [1–3]. Glucose plays an important role in the human metabolic process and especially the glucose concentration in blood or urine is often used as an important indicator for the diagnosis of diabetes [4]. Consequently, the reliable and easy-to-operate detections of H_2O_2 and glucose are of great importance due to their vital function. Enzymatic assay have obtained significant achievements in reliable quantification of H_2O_2 and glucose owing to their high sensitivity and selectivity [5]. However, some unfavorable factors for enzyme-based assay limit their wide applications, such as easy deactivation, the strong influence of pH and humidity, and high cost [6]. To overcome the issues, considerable efforts have been devoted to the non-enzymatic assay with excellent detection performances.

Electrochemical detection based on highly active electrocatalysts furnishes great application prospects towards H_2O_2 and glucose assay due to its traits of high sensitivity, compatibility, and simple operation [7–10]. For H_2O_2 and glucose assay, the sensitivity and selectivity mostly depend on the electrocatalytic activity and electron conductivity of the catalysts [4, 11]. Hence, the design and preparation of fascinating catalysts with desirable electrochemical performance are of great significance to achieve their highly sensitive detections. A variety of nanomaterials, such as noble metals [12], other transition metals [6] and their compounds [13], have been extensively employed in the H_2O_2 and glucose detection. However, the requirement of alkaline working condition for most catalysts in glucose detection restricts their practical applications [4]. Among various catalysts, Pt nanomaterials arouse great research interests by virtue of the unique catalytic performances, high electron conductivity, and neutral application condition [14]. Nonetheless, the most severe problem of the monometallic Pt lies in its poor anti-

Electronic supplementary material The online version of this article (https://doi.org/10.1007/s00604-019-3728-7) contains supplementary material, which is available to authorized users.

✉ Caixia Xu
chm_xucx@ujn.edu.cn

✉ Jiagang Hou
hjg@qlu.edu.cn

[1] Institute for Advanced Interdisciplinary Research, School of Chemistry and Chemical Engineering, University of Jinan, Jinan 250022, Shandong Province, China

[2] Qilu University of Technology (Shandong Academy of Sciences), Jinan 250353, Shandong Province, China

poisoning capacity during the catalytic process [15]. One of the most effective approaches to optimize the electrocatalytic performances of Pt is introducing other assistant metal to form the bimetallic alloy [16]. The secondary metal is not only helpful to reduce the cost of Pt-based electrocatalysts but also significantly promote the electrocatalytic and detection performances by modifying the d-band center of Pt [17]. Impressively, as a typical transition metal, Cu is considered as one of the best assistant metal candidates on account of its intrinsic electrocatalytic properties [18] and prominent synergistic catalytic effect with noble metal catalysts [19]. Ye et al. fabricated the PtCu yolk-shell alloy cubes using Cu_2O cubes as templates. Relative to Pt/C catalyst, the PtCu alloy displayed improved catalytic activity and durability for methanol electrooxidation [20]. Yan demonstrated the synthesis of ultrathin PtCu nanowires grown over reduced graphene oxide, which presented excellent electrocatalytic activity for oxygen reduction reaction [17]. Peng et al. synthesized the highly dispersed PtCu nanoparticles on nitrogen-doped graphene, which exhibited remarkably enhanced electrocatalytic performance and high tolerance to CO poisoning toward the methanol electrooxidation [21].

Apart from the composition, the morphology of electrocatalyst also plays an important role in the electrocatalytic process. The nanoporous structure has attracted enormous research attention owing to the fantastic structural merits of abundant surface active sites and fluent mass transport pathway. In particular, the dealloying strategy has been proved to be a powerful method to scale up the preparation of nanoporous metallic materials [22]. Based on the above considerations, the multimodal nanoporous PtCu (np-PtCu) flowers is fabricated via selective dissolution of Al followed by the partial Cu from PtCuAl precursor alloy at mild condition in current work. Upon the two-step dealloying, multiscale pores and ligaments are successfully produced through the entire interlinking flower-like composite. The integral skeleton and interconnected hollow channels in the np-PtCu alloy furnish the structure foundation for high electron conductivity, smooth pathway for easy mass transport, and sufficient reactive sites during the electrocatalytic process. Thanks to the specific nanoporous architecture, rich electroactive sites, and strong synergistic catalytic effect of Cu to Pt, the np-PtCu alloy displays the superior electrocatalytic activity and excellent detection performance in neutral solution. The assay method based the np-PtCu exhibits high sensitivity, outstanding selectivity, broad linear concentration range, and long-term detection durability towards H_2O_2 and glucose assay.

Experimental

Reagents and materials

The np-PtCu alloy was prepared as described in our previous work [23]. $Pt_{2.5}Cu_{14.5}Al_{83}$ alloy were prepared by refining high-purity (>99.9%) Pt, Cu, and Al metals in an arc-furnace. The alloy foils were obtained through the melt-spinning under an Ar-protected atmosphere. Np-PtCu alloy was prepared by etching PtCuAl source alloy foils in 0.5 M NaOH for 48 h followed by the further treatment in 1 M HNO_3 for 30 min at the room temperature.

H_2O_2 solution (30 wt%), glucose, Na_2HPO_4, and KH_2PO_4 were purchased from Sinopharm Chemical Reagent Co. Ltd. (https://www.reagent.com.cn/). The phosphate buffered saline (0.1 M PBS, pH 7.0) solution was made by mixing the 0.1 M Na_2HPO_4 and 0.1 M KH_2PO_4 with the volume ration of ~4: 6. Dopamine (DA), acetaminophen (AC), and ascorbic acid (AA) were obtained from Sigma-Aldrich (https://www.sigmaaldrich.com/). The commercial Johnson-Matthey Pt/C catalyst (20 wt.%) was supplied by Alfa Aesar (https://www.alfa.com/zh-cn/). All chemicals were analytically pure and directly used without treatment. Ultra-pure water (18.2 MΩ cm) was used in all experimental procedures and measurements.

Instruments and measurements

Powder X-ray diffraction (XRD) patterns were acquired on a Bruker D8 advanced X-ray diffractometer using Cu Kα radiation at a step rate of $0.04^{\circ}\cdot s^{-1}$. The microstructure of sample was characterized on a JEM-2100 Transmission Electron Microscope (TEM) and a JSM-6700 Field Emission Scanning Electron Microscope (SEM) equipped with an Oxford INCA X-sight Energy Dispersive X-ray Spectrometer (EDS). X-ray photoelectron spectra (XPS) were carried out on a X-ray photoelectron spectrometer (ESCALAB 250) using the Monochromated Al Ka X-ray as the excitation source. N_2 adsorption-desorption isotherms were examined on a QuadraSorb SI at 77.3 K. The surface areas were calculated via the Brunauer-Emmett-Teller (BET) method. The pore size distribution was obtained from desorption branch through the Barrett-Joyner-Halenda (BJH) method. The electrochemical measurements were performed on a standard three-electrode CHI 760D electrochemical workstation, with a glassy carbon electrode as the working electrode, a mercury-mercuric sulfate electrode as the reference electrode, and a Pt electrode as the counter electrode. All potentials were provided according to the reversible hydrogen electrode (RHE) scale for clarity. The electrochemical surface areas of the Pt-based catalysts were calculated by integrating the reduction charges during the stripping of surface monolayer oxide in N_2-purged 0.5 M H_2SO_4 solution, in which the used charge density is 210 μC cm^{-2} Pt [24]. The current density is normalized through dividing the current by the electrochemical active surface area of Pt-based catalysts.

Preparation of the modified electrodes

1.5 mg of np-PtCu sample powder, 1.0 mg of carbon powder, 300 μL ethanol and 100 μL Nafion solution (0.5 wt.%) were mixed to form a uniform catalyst ink under ultrasonic conditions. A working electrode was modified by adding 3 μL of catalyst ink to the surface of a clean and polished glassy carbon electrode.

Results and discussion

Characterization of the np-PtCu alloy

The morphology and detailed structure of the resulting sample upon two-step dealloying of PtCuAl alloy was first characterized. As displayed in Fig. 1a, the dealloyed product exhibited the nanospongy morphology composed of interconnected flowers. From Fig. 1b, it can be observed that each flower consisted of multiple assembled nanorods with the diameter around 70 nm. Impressively, there are numerous interconnected tiny pores uniformly distributed in the nanorods. The TEM image in Fig. 1c also confirms the generation of flower-like structure with high porosity, where the obvious big and small bright regions indicate the multimodal pore size distributions. The large pores with the size of 5–8 nm result from the dissolution of Al in the NaOH solution, while the tiny pores (2–4 nm) in the nanorod-like petals are generated upon the following dissolution of Cu in HNO_3 solution. From Fig. 1d, the highly ordered lattice fringes with a period of 0.225 nm correspond to the (111) crystal plane of PtCu alloy [21]. It is clear that the two-step dealloying of PtCuAl alloy successfully generate the multimodal porous architecture with the integral interconnected network backbone, which is benificial for the fluent mass transport and full contact with the surface active sites during the electrocatalytic process.

XRD was performed to examine the crystal structure of the dealloyed sample. As shown in Fig. 2a, the dealloyed product presents three diffraction peaks at 41.9, 48.8, and 71.1 (2θ), which can be assigned to (111), (200), and (220) crystal planes of the face centered cubic PtCu alloy. All diffraction peaks of the resulting PtCu alloy locate just between standard diffraction peaks of pure Pt and Cu with no other peaks observed, demonstrating the successful preparation of homogeneous single-phase PtCu alloy [22]. The EDS data in Fig. 2b indicates that the atomic composition of the np-PtCu is about $Pt_{63}Cu_{37}$.

XPS and BET analysis were further carried out to determine the detail structures of the dealloyed samples. As shown in Fig. S1a, two peaks locating at 71.5 and 74.8 eV correspond to Pt $4f_{7/2}$ and Pt $4f_{5/2}$ [22], indicating that metallic Pt^0 is the dominant state in the PtCu alloy [25]. The peaks at 932.4 and 953.2 eV are assigned to Cu $2p_{3/2}$ and Cu $2p_{1/2}$, revealing the

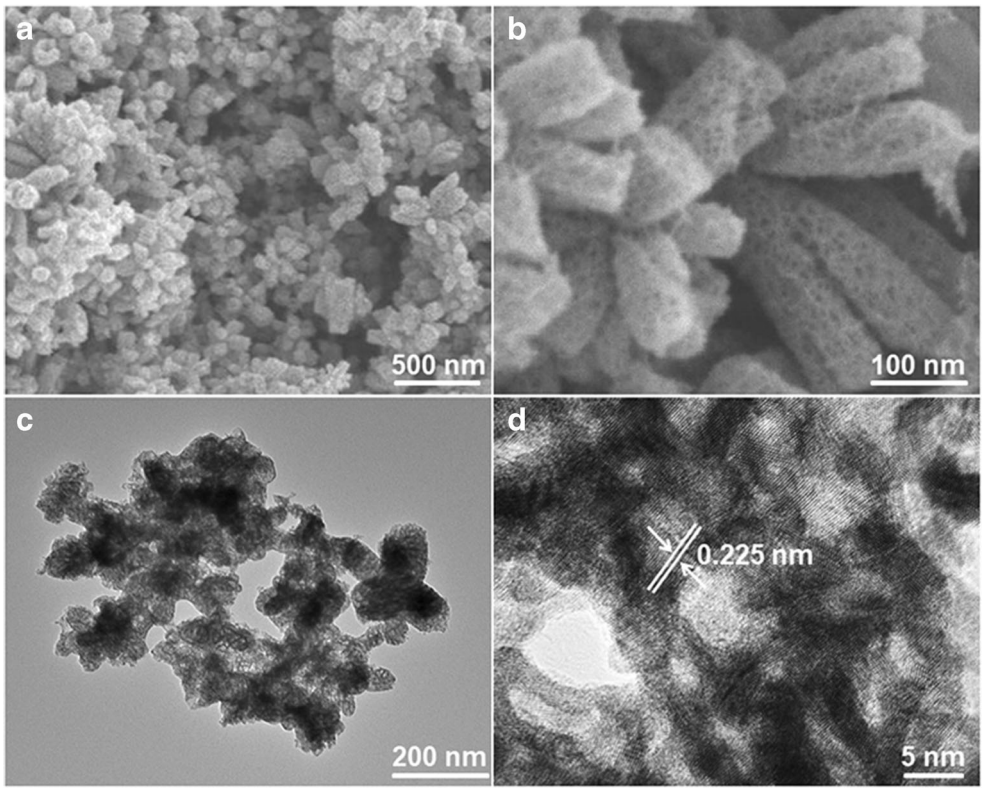

Fig. 1 SEM images (**a**, **b**) and TEM images (**c**, **d**) of the dealloyed sample upon etching PtCuAl alloy in 0.5 M NaOH for 48 h followed by further treatment in 1 M HNO_3 for 30 min at the room temperature

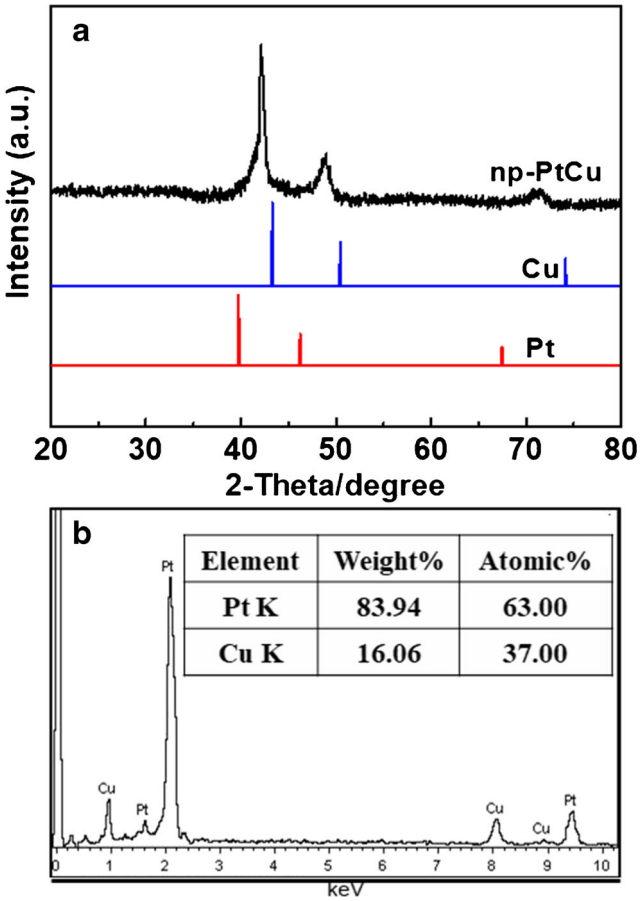

Fig. 2 XRD patterns (**a**) and EDS data (**b**) of the dealloyed sample

presence of metallic Cu^0 as well as a small amount of Cu(I) and Cu(II) [22, 25, 26]. The XPS result suggests that the dealloyed sample is mainly comprised of Pt^0 and Cu^0 metal. The co-existence of Cu oxygen species on the surface of the PtCu alloy may stem from the oxidation of surface Cu atoms [22]. Multimodal np-PtCu shows a high specific surface area with the value ~43.6 $m^2\ g^{-1}$. The large surface area of the np-PtCu comes from the multiscale porous architecture, which provides the sufficient active sites for the electrochemical oxidation reaction and improves the sensitivity of electrochemical detection of H_2O_2 and glucose. The np-PtCu alloy presents a sharp and strong peak at 2–8 nm in the pore size distribution, which is in good agreement with the TEM result (Fig. 1c and Fig. 1d).

Electrochemical detection of hydrogen peroxide by using the np-PtCu alloy

Np-PtCu possesses the advanced nanostructure with rich pore openings and interconnected nanoscaled ligaments, which is especially preferable for the easy mass transport and high electron conductivity in the electrocatalytic process. The potential application in H_2O_2 detection of np-PtCu was first investigated by cyclic voltammetric (CV) method. Figure 3a&b present the typical CVs of np-PtCu modified electrode in PBS (pH 7.0) solution in the presence and absence of 5 mM H_2O_2 with those of Pt/C for comparison. After the addition of 5 mM H_2O_2 in PBS solution, intense oxidation current starting from 0.43 V was observed on the np-PtCu (Fig. 3a). By contrast, Pt/C exhibits slightly increased oxidation current in the presence of 5 mM H_2O_2 (Fig. 3b). It is clear that np-PtCu shows much higher catalytic activity than Pt/C toward H_2O_2 electrooxidation in the wide potential range of 0.5 to 1.2 V. The onset oxidation potential of np-PtCu negatively shifted more than 170 mV compared with Pt/C catalysts.

Figure 3c shows the typical amperometric responses of np-PtCu and Pt/C modified electrodes upon successive addition of H_2O_2 into the stirring PBS solution under the constant potential of 0.7 V. Both np-PtCu and Pt/C present obvious increased current density immediately after the addition of H_2O_2. However, np-PtCu reaches the maximum current response within the shorter period relative to Pt/C and particularly the much higher current response on np-PtCu indicates its superior sensitivity. The Pt/C modified electrode shows linear responses to H_2O_2 in the concentration range of 0.01–1.3 mM with the detection limit of 0.3 μM ($S/N = 3$). The np-PtCu catalyst exhibits linear relationship in the broader range of 0.01–1.7 mM (linear equation: $y = 64.7x + 4.87$, $R^2 = 0.998$) with the sensitivity of 64.7 $\mu A \cdot mM^{-1} \cdot cm^{-2}$ and a lower detection limit of 0.1 μM (S/N = 3). It is evident that np-PtCu presents higher sensitivity, more rapid response, wider linear concentration range, and lower detection limit. The efficient electrooxidation of H_2O_2 on the np-PtCu is considered to stem from the synergistic alloy effect between Pt and Cu as well as the specific architecture with interlinking pore and ligament channels. The detection performances of np-PtCu also show certain superiorities over some reported assay methods toward H_2O_2 as shown in Table 1 [24, 27–30], from which higher sensitivity and lower detection limit in certain concentration range were observed for np-PtCu.

Electrochemical detection of glucose by using the np-PtCu alloy

The electrocatalytic performances of np-PtCu toward glucose oxidation were also tested to evaluate its potential application in glucose detection. Figure 4a&b give the CVs of the np-PtCu and commercial Pt/C modified electrodes in PBS solution (pH 7.0) with and without 10 mM glucose. It is clear to find that the current density of glucose electrooxidation on np-PtCu alloy is almost 20 times that of the commercial Pt/C catalyst in the positive scan. As displayed in Fig. 4a, two strong oxidation peaks at 0.05 and 0.45 V were observed over np-PtCu alloy in the presence of 10 mM glucose. The first oxidation peak at 0.05 V comes from the electrochemical adsorption of glucose molecules, which will generate the oxidation current and thereby produce the adsorbed glucose-related

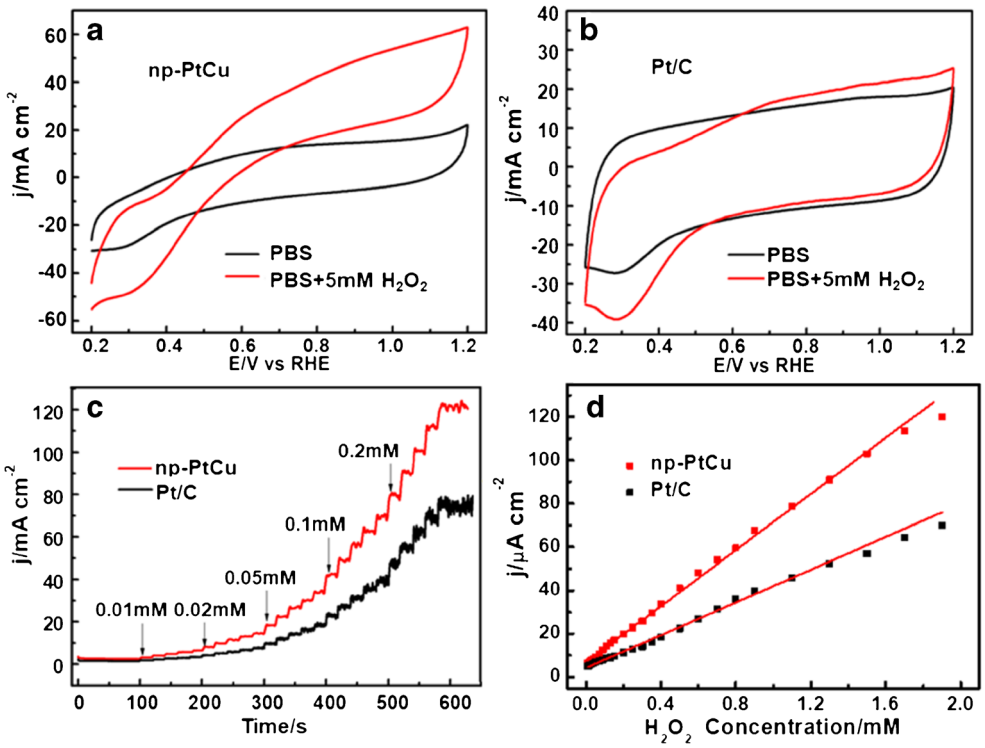

Fig. 3 CV curves of (**a**) np-PtCu, (**b**) Pt/C in PBS solution and PBS solution with 5 mM H_2O_2 at 50 mV/s, (**c**) Amperometric responses of np-PtCu and Pt/C electrodes upon successive injection of H_2O_2 into stirring PBS solution at 0.7 V, (**d**) Plots of response currents vs. H_2O_2 concentrations

intermediates [31]. Along with the reaction proceeds, the current density decreases because the accumulation of the intermediates on the electrode surface blocks the electrochemical adsorption of glucose and further suppresses the glucose oxidation. Further increasing the potential to 0.2 V, Pt-OH species start to produce on the catalyst surface, which promotes the intermediates oxidation and generates the increased oxidation current in the range of 0.2–0.7 V [24]. In the negative scanning process, since the fresh Pt metallic surface is re-exposed by the reduction of the oxidized Pt surface, more active sites is available for the glucose oxidation, leading to the large anodic peak at the potential around 0.4 V. As the backward scan continues, the accumulation of intermediates occurs again, resulting in the current decay. Pt/C catalysts exhibit relatively lower oxidation current in the presence of glucose with no distinct oxidation peaks similar to np-PtCu observed. The superior electrooxidation activity of glucose on np-PtCu alloy illustrates that the reaction kinetics for glucose oxidation was dramatically optimized due to its multimodal porous architecture and the synergistic effect between Pt and Cu.

The detection performance of np-PtCu alloy was further examined by amperometric detection upon the continuous addition of glucose at 0.4 V, including the responses of Pt/C catalyst for comparison (Fig. 4c). Upon the addition of glucose np-PtCu alloy exhibits stronger current responses than those of Pt/C catalyst, indicating the superior sensitivity of np-PtCu alloy. As depicted in Fig. 4d, the np-PtCu exhibits broad linear concentration

Table 1 Analytical parameters of different electrochemical assay toward H_2O_2

Electrode Materials	Linear range (mM)	Detection limit (μM)	Ref.
PtAu [a]	0.05–2.75	0.1	[24]
Pt NPs-CDs/IL-GO [b]	0.001–0.9	0.1	[27]
Pt-DENs/CNTs/GCE [c]	0.003–0.4	0.8	[28]
PB/nanopores [d]	3×10^{-3}-2.1×10^{-2}	0.6	[29]
Co_3O_4/MWCNTs [e]	0.02–0.43	2.46	[30]
np-PtCu [f]	0.01–1.7	0.1	This work

[a] nanoporous platinum-gold alloy; [b] Pt nanoparticles-carbon quantum dots/ionic liquid functionalized graphene oxide; [c] dendrimer-encapsulated Pt nanoclusters and carbon nanotubes; [d] Prussian blue/sol-gel composite; [e] Cobalt oxide nanoparticles anchored to multiwalled carbon nanotubes; [f] nanoporous PtCu alloy

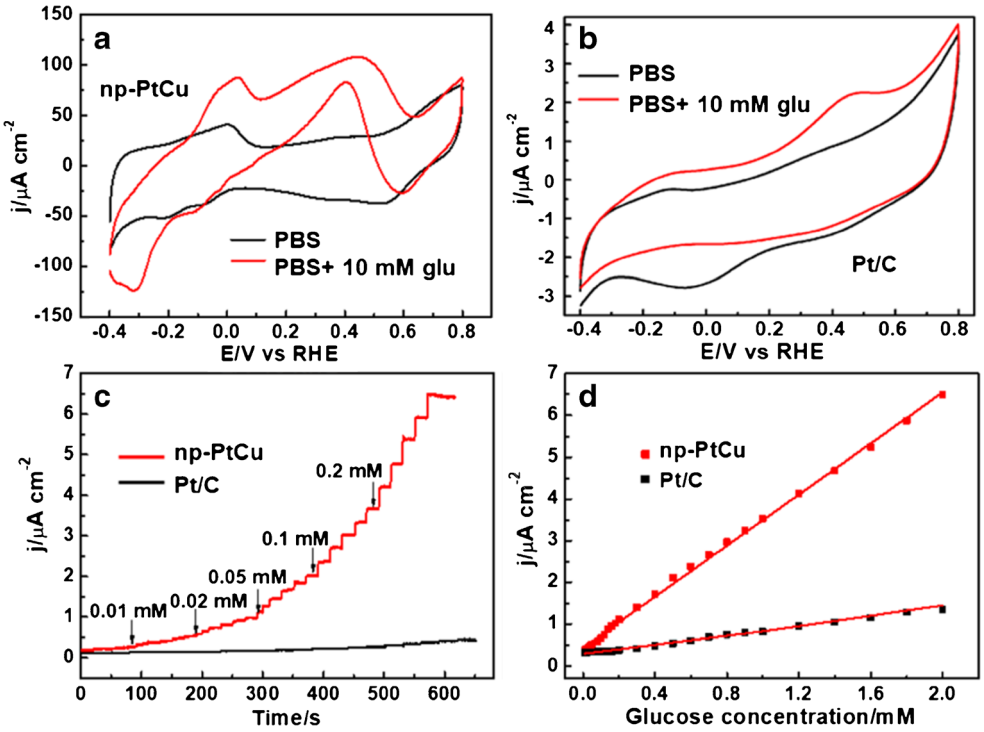

Fig. 4 CV curves of (**a**) np-PtCu, (**b**) Pt/C in PBS solution and PBS solution with 10 mM glucose at 50 mV/s, (**c**) Amperometric responses of np-PtCu and Pt/C electrodes upon successive addition of glucose into stirring PBS solution at 0.4 V, (d) Plots of response currents vs. glucose concentrations

range of 0.01–2.0 mM (linear equation: $y = 3.16\ x + 0.37$, $R^2 = 0.999$), high sensitivity of 3.16 μA·mM^{-1}·cm^{-2}, and lower detection limit of 0.1 μM than Pt/C (S/N = 3). The remarkable detection performances of np-PtCu toward glucose detection are also superior to that of other reported data as shown in Table 2 [4, 19, 24, 32, 33].

The durability for the detection of H_2O_2 and glucose by using the np-PtCu alloy

Long-term detection durability is an important parameter to evaluate the practical application potential for the used assay method. The potentiostatic method was carried out to monitor the continuous detection stability of np-PtCu alloy for H_2O_2 and glucose. After the uninterrupted running as long as 4000 s in PBS solution with 0.5 mM H_2O_2 at 0.7 V, ~90% of the initial current response was remained over np-PtCu alloy, while 65% was maintained on the Pt/C catalysts (Fig. 5a). In addition, the amperometric response over np-PtCu is dramatically intense compared with that of Pt/C, confirming its wonderful sensitivity for hydrogen peroxide detection. As shown in Fig. 5b, even after running for 4000 s, 91% of the initial current was kept over the np-PtCu alloy in 5.0 mM glucose. By comparison, the oxidation current on Pt/C underwent severe decay with only 62% retained. The more stable and sustained current output than Pt/C suggests that the incorporation of Cu and the specific multiscaled porous architecture endow np-PtCu much enhanced detection durability as well as the anti-poisoning stability for the H_2O_2 and glucose detection.

Table 2 Analytical parameters of different electrochemical assay toward glucose

Electrode Materials	Linear range (mM)	Detection limit (μM)	Supporting electrolyte	Ref.
Pt/Au/BDD [a]	0.01–7.5	7.7	0.1 M PBS + 0.1 M NaCl	[4]
PtNi [b]	5–40	0.35	PBS	[19]
PtAu [c]	0.2–5.4	0.5	PBS	[24]
Cu_3P NW/CF [d]	0.05–1	0.329	0.1 M NaOH	[32]
Co NBs/rGO [e]	0.15–6.25	47.5	0.1 M NaOH	[33]
np-PtCu [f]	0.01–2.0	0.1	PBS	This work

[a] bimetallic Pt/Au nanocatalyst on the surface of a boron-doped diamond electrode; [b] monodisperse stone-like PtNi alloy nanoparticles; [c] nanoporous PtAu alloy; [d] copper phosphide nanowire on copper foam; [e] Porous Co nanobeads/rGO nanocomposites; [f] nanoporous PtCu alloy

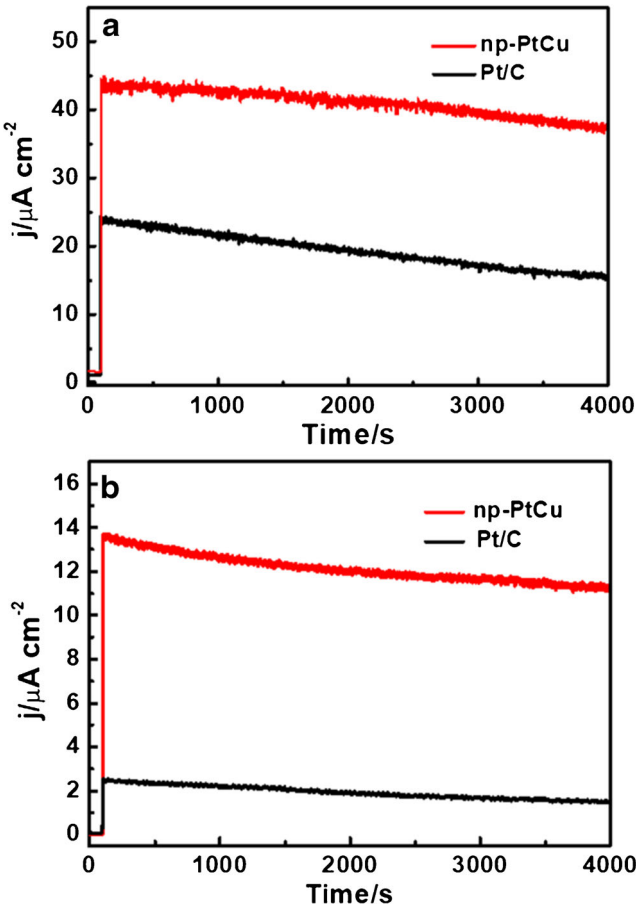

Fig. 5 Amperometric currents of np-PtCu and Pt/C catalysts in a stirring PBS solution with (**a**) 0.5 mM H_2O_2 for 4000 s at 0.7 V, (**b**) 5.0 mM glucose for 4000 s at 0.4 V

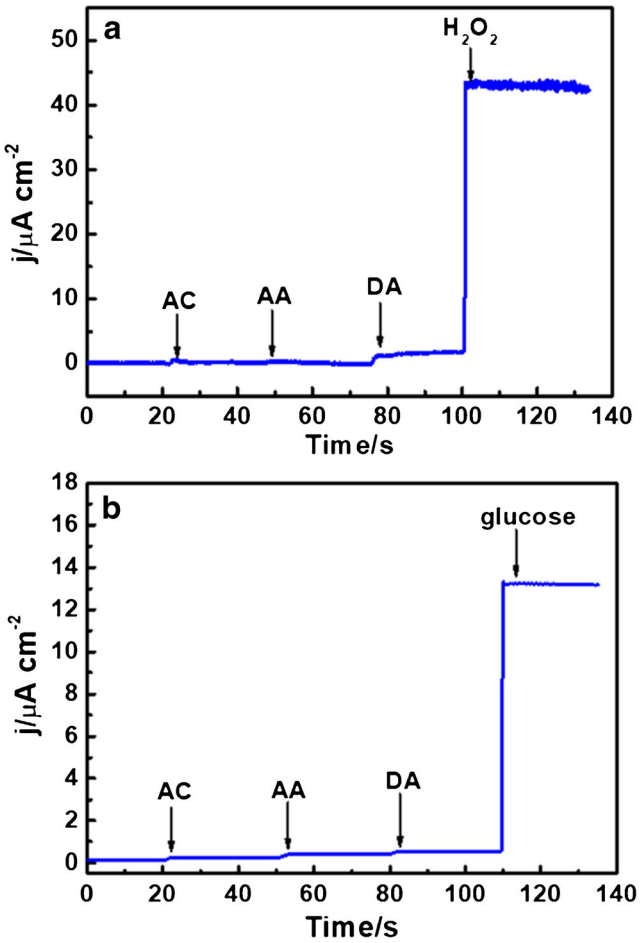

Fig. 6 Amperometric responses to the successive injection of 0.04 mM AC, 0.2 mM AA, and 0.01 mM DA on np-PtCu alloys in a stirring PBS solution followed by the addition of 0.5 mM H_2O_2 at 0.7 V (**a**) and 5.0 mM glucose at 0.4 V (**b**)

Selectivity for H_2O_2 and glucose

The selectivity of np-PtCu alloy is another key factor to estimate its application prospect. It is well known that H_2O_2 and glucose usually coexists with some compounds such as AA, DA, and AC, which may generate the interfering electrochemical signals at the applied detection potential [34]. As shown in Fig. 6, the amperometric responses of np-PtCu modified electrode upon the successive addition of electroactive species in to PBS solution were monitored. Tiny current response was recorded after the addition of 0.04 mM AC, 0.2 mM AA, and 0.01 mM DA (Fig. 6a). The prominent current increase after the addition of 0.5 mM H_2O_2 suggests that the np-PtCu alloy possesses excellent selectivity towards H_2O_2 at 0.7 V. Additionally, the response current towards AA, DA, and AC generated on np-PtCu can be ignored compared with the electrochemical signals caused by 5.0 mM glucose at 0.4 V. Based on the experimental observations above, it is conclusive that np-PtCu alloy presents the outstanding selectivity, revealing its high anti-poisoning ability toward some coexisted electroactive species.

Analysis of real samples

The preparation of the electrodes before the electrochemical test

The glassy carbon electrodes were modified with np-PtCu alloy according to the way shown in the 2.3 section. After the modified electrodes were dried naturally at room temperature, the standard three-electrode electrochemical workstation was assembled for the electrochemical measurement. The electrochemical surface areas of the electrodes were calculated through the method presented in the 2.2 section.

The preparation of the solutions

Proper volume of the real sample solution was dispersed into the PBS solution under stirring to get the tested solution. The preparation method of the PBS solution was provided in the 2.1 section. The principle of real samples dosage is to treat the concentration of tested solution within the linear range through dispersing the real sample into PBS solution. That is to say, the concentrations of the target solutions should be within 0.01 to 1.7 mM for H_2O_2 detection and 0.01 to 2.0 mM for glucose detection.

The assay

The modified working electrode was dipped into the tested solution under the stirring. The working voltages were set as 0.4 V for the H_2O_2 detection and 0.7 V for glucose detection according to the RHE scale. The amperometric responses can be normalized to the current density through dividing the detected current by the electrochemical active surface area. The concentration of the tested solution can be tuned by dilution or concentrating to make the value of current density within the range of 4.93–114.8 $\mu M \cdot cm^{-2}$ for H_2O_2 detection. 4.93 $\mu M \cdot cm^{-2}$ is the current density of the minimum H_2O_2 concentration in linear concentration (0.01 mM) and 114.8 $\mu M \cdot cm^{-2}$ is the current density of the maximum H_2O_2 concentration in linear concentration (1.7 mM). The range of current density is 0.4–6.69 $\mu M \cdot cm^{-2}$ for glucose detection, which is the corresponding current density of glucose in linear concentration (0.01–2.0 mM). The exact concentration of H_2O_2 or glucose in the real samples can be calculated through the linear equations ($y = 64.7\ x + 4.87$, $R^2 = 0.998$ for H_2O_2 detection and $y = 3.16\ x + 0.37$, $R^2 = 0.999$ for glucose detection; y presents the current density, typical unit of which is $\mu M \cdot mM^{-1} \cdot cm^{-2}$; x presents the concentration of H_2O_2 or glucose, typical unit of which is mM).

Conclusions

Interconnected flower-like nanoporous PtCu alloy with multiscaled pore size distribution are successfully fabricated by a mild two-step dealloying process in this work. The np-PtCu alloy exhibits typical characteristics of strong synergistic effect between Pt and Cu, favorable hierarchical porous architecture, as well as the modified charge transfer kinetics in the electrocatalytic reaction. More important, the assay method based on np-PtCu alloy achieves highly sensitive, selective, and long-term detection of H_2O_2 and glucose. The developed strategy with merits of scalable preparation, good reproducibility, and no use of any organic solvent endows it suitable for the fabrication of other nanoporous alloys.

Acknowledgements This work was supported by National Natural Science Foundation of China (51772133), Natural Science Foundation of Shandong Province (ZR2017JL022), and the program for Taishan Scholar of Shandong province (ts201712048).

Compliance with ethical standards There are no potential conflicts of interest.

References

1. Vogna D, Marotta R, Napolitano A, Andreozzi R, d'Ischia M (2004) Advanced oxidation of the pharmaceutical drug diclofenac with UV/H_2O_2 and ozone. Water Res 38:414–422
2. Opazo C, Huang X, Cherny RA (2002) Metalloenzyme-like activity of Alzheimer's disease beta-amyloid. Cu-dependent catalytic conversion of dopamine, cholesterol, and biological reducing agents to neurotoxic H_2O_2. J Biol Chem 277:40302–40308
3. Bokare AD, Choi W (2014) Review of iron-free Fenton-like systems for activating H_2O_2 in advanced oxidation processes. J Hazard Mater 275:121–135
4. Nantaphol S, Watanabe T, Nomura N, Siangproh W, Chailapakul O, Einaga Y (2017) Bimetallic Pt-Au nanocatalysts electrochemically deposited on boron-doped diamond electrodes for nonenzymatic glucose detection. Biosens Bioelectron 98:76–82
5. Tang Y, Liu Q, Jiang Z, Yang X, Wei M, Zhang M (2017) Nonenzymatic glucose sensor based on icosahedron AuPd@CuO core shell nanoparticles and MWCNT. Sensors Actuators B Chem 251:1096–1103
6. Jia L, Wei X, Lv L, Zhang X, Duan X, Xu Y, Liu K, Wang J (2018) Electrodeposition of hydroxyapatite on nickel foam and further modification with conductive polyaniline for non-enzymatic glucose sensing. Electrochim Acta 280:315–322
7. Hwang D, Lee S, Seo M, Chung DT (2018) Recent advances in electrochemical non-enzymatic glucose sensors-a review. Anal Chim Acta 1033(1–34):1–34
8. Wei P, Gan T, Wu K (2018) N-methyl-2-pyrrolidone exfoliated graphene as highly sensitive analytical platform for carbendazim. Sensors Actuators B Chem 274:551–559
9. Gan T, Zhao A, Wang Z, Liu P, Sun J, Liu Y (2017) An electrochemical sensor based on SiO_2@TiO_2-embedded molecularly imprinted polymers for selective and sensitive determination of theophylline. J Solid State Electrochem 21:3683–3691
10. Gan T, Lv Z, Sun Y, Shi Z, Sun J, Zhao A (2016) Highly sensitive and molecular selective electrochemical sensing of 6-benzylaminopurine with multiwall carbon nanotube@SnS_2-assisted signal amplification. J Appl Electrochem 46:389–401
11. Bai Z, Dong W, Ren Y, Zhang C, Chen Q (2018) Preparation of nano au and Pt alloy microspheres decorated with reduced graphene oxide for nonenzymatic hydrogen peroxide sensing. Langmuir 34: 2235–2244
12. Mei H, Wang X, Zeng T, Huang L, Wang Q, Ru D, Huang T, Tian F, Wu H, Gao J (2019) A nanocomposite consisting of gold nanobipyramids and multiwalled carbon nanotubes for amperometric nonenzymatic sensing of glucose and hydrogen peroxide. Microchim Acta 186:235–242
13. Gao Y, Yang F, Yu Q, Fan R, Yang M, Rao S, Lan Q, Yang Z, Yang Z (2019) Three-dimensional porous Cu@Cu_2O aerogels for direct voltammetric sensing of glucose. Microchim Acta 186:192–200
14. Chen C, Ran R, Yang Z, Lv R, Shen W, Kang F, Huang Z (2018) An efficient flexible electrochemical glucose sensor based on carbon nanotubes/carbonized silk fabrics decorated with Pt microspheres. Sensors Actuators B Chem 256:63–70

15. Hu Y, Niu X, Zhao H, Tang J, Lan M (2015) Enzyme-free amperometric detection of glucose on platinum-replaced porous copper frameworks. Electrochim Acta 165:383–389
16. Fu Y, Huang D, Li C, Zou L, Ye B (2013) Graphene blended with SnO_2 and Pd-Pt nanocages for sensitive nonenzymatic electrochemical detection of H_2O_2 released from living cells. Anal Chim Acta 1014:10–18
17. Yan X, Chen Y, Deng S, Yang Y, Huang Z, Ge C, Xu L, Sun D, Fu G, Tang Y (2017) In situ integration of ultrathin PtCu nanowires with reduced graphene oxide nanosheets for efficient electrocatalytic oxygen reduction. Chem-Eur J 23:16871–16876
18. Huang J, Dong Z, Li Y, Li J, Wang J, Yang H, Li S, Guo S, Jin J, Li R (2013) High performance non-enzymatic glucose biosensor based on copper nanowires-carbon nanotubes hybrid for intracellular glucose study. Sensors Actuators B Chem 182:618–624
19. Wang R, Liang X, Liu H, Cui L, Zhang X, Liu C (2018) Non-enzymatic electrochemical glucose sensor based on monodispersed stone-like PtNi alloy nanoparticles. Microchim Acta 185:339–345
20. Ye S, He X, Ding L, Pan Z, Tong Y, Wu M, Li G (2014) Cu_2O template synthesis of high-performance PtCu alloy yolk-shell cube catalysts for direct methanol fuel cells. Chem Commun 50:12337–12340
21. Peng X, Chen D, Yang X, Wang D, Li M, Tseng CC, Panneerselvam R, Wang X, Hu W, Tian J, Zhao Y (2016) Microwave-assisted synthesis of highly dispersed PtCu nanoparticles on three-dimensional nitrogen-doped graphene networks with remarkably enhanced methanol electrooxidation. ACS Appl Mater Interfaces 8:33673–33680
22. Qiu H, Xu H, Li X, Wang J, Wang Y (2015) Core-shell-structured nanoporous PtCu with high Cu content and enhanced catalytic performance. J Mater Chem A 3:7939–7944
23. Zhou Q, Qi L, Yang H, Xu C (2018) Hierarchical nanoporous platinum-copper alloy nanoflowers as highly active catalysts for the hydrolytic dehydrogenation of ammonia borane. J Colloid Interface Sci 513:258–265
24. Wang J, Gao H, Sun F, Xu C (2014) Nanoporous PtAu alloy as an electrochemical sensor for glucose and hydrogen peroxide. Sensors Actuators B Chem 191:612–618
25. Fu S, Zhu C, Shi Q, Xia H, Du D, Lin Y (2016) Highly branched PtCu bimetallic alloy nanodendrites with superior electrocatalytic activities for oxygen reduction reactions. Nanoscale 8:5076–5081
26. Ghodselahi T, Vesaghi M, Shafiekhani A, Baghizadeh A, Lameii M (2008) XPS study of the $Cu@Cu_2O$ core-shell nanoparticles. Appl Surf Sci 255:2730–2734
27. Chen D, Zhuang X, Zhai J, Zheng Y, Lu H, Chen L (2018) Preparation of highly sensitive Pt nanoparticles-carbon quantum dots/ionic liquid functionalized graphene oxide nanocomposites and application for H_2O_2 detection. Sensors Actuators B Chem 255:1500–1506
28. Liu J, Ding S (2017) Non-enzymatic amperometric determination of cellular hydrogen peroxide using dendrimer-encapsulated Pt nanoclusters/carbon nanotubes hybrid composites modified glassy carbon electrode. Sensors Actuators B Chem 251:200–207
29. Doroftei F, Pinteala T, Arvinte A (2014) Enhanced stability of a Prussian blue/sol-gel composite for electrochemical determination of hydrogen peroxide. Microchim Acta 181:111–120
30. Heli H, Pishahang J (2014) Cobalt oxide nanoparticles anchored to multiwalled carbon nanotubes: synthesis and application for enhanced electrocatalytic reaction and highly sensitive nonenzymatic detection of hydrogen peroxide. Electrochim Acta 123:518–526
31. Tominaga M, Nagashima M, Nishiyama K, Taniguchi I (2007) Surface poisoning during electrocatalytic monosaccharide oxidation reactions at gold electrodes in alkaline medium. Electrochem Commun 9:1892–1898
32. Xie L, Asiri AM, Sun X (2017) Monolithically integrated copper phosphide nanowire: an efficient electrocatalyst for sensitive and selective nonenzymatic glucose detection. Sensors Actuators B Chem 244:11–16
33. Song Y, Wei C, He J, Li X, Lu X, Wang L (2015) Porous Co nanobeads/rGO nanocomposites derived from rGO/Co-metal organic frameworks for glucose sensing. Sensors Actuators B Chem 220:1056–1063
34. Zhong S, Zhuang J, Yang D, Tang D (2017) Eggshell membrane-templated synthesis of 3D hierarchical porous au networks for electrochemical nonenzymatic glucose sensor. Biosens Bioelectron 96:26–32